

# Sensory organ like response determines the magnetism of zigzag-edged honeycomb nanoribbons

Somnath Bhowmick<sup>1,\*</sup>, Amal Medhi<sup>2,†</sup> and Vijay B Shenoy<sup>2‡</sup>

<sup>1</sup>*Materials Research Center, Indian Institute of Science, Bangalore 560 012, India*

<sup>2</sup>*Centre for Condensed Matter Theory, Department of Physics,  
Indian Institute of Science, Bangalore 560 012, India*

(Dated: August 17, 2012)

We present an *analytical* theory for the magnetic phase diagram for zigzag edge terminated honeycomb nanoribbons described by a Hubbard model with an interaction parameter  $U$ . We show that the edge magnetic moment varies as  $\ln U$  and uncover its dependence on the width  $W$  of the ribbon. The physics of this owes its origin to the sensory organ like response of the nanoribbons, demonstrating that considerations beyond the usual Stoner-Landau theory are necessary to understand the magnetism of these systems. A first order magnetic transition from an anti-parallel orientation of the moments on opposite edges to a parallel orientation occurs upon doping with holes or electrons. The critical doping for this transition is shown to depend inversely on the width of the ribbon. Using variational Monte-Carlo calculations, we show that magnetism is robust to fluctuations. Additionally, we show that the magnetic phase diagram is generic to zigzag edge terminated nanostructures such as nanodots. Furthermore, we perform first principles modeling to show how such magnetic transitions can be realized in substituted graphene nanoribbons.

PACS numbers: 75.75.-c, 73.20.-r, 75.70.-i, 73.22.Pr

Interest and activity in magnetic nanostructures has been driven by their possible application in nanoelectronic/spintronic devices, with graphene based systems grabbing a significant fraction of the attention.[1] The remarkable electronic properties of graphene[2, 3] with a Dirac like spectrum have made it a suitable candidate for many applications.[4–7] From a theoretical perspective, electron interactions and correlations effects on the honeycomb lattice contain many interesting phenomena[8] including magnetism[9] and superconductivity.[10]

Magnetism at the zigzag terminated edges of graphene has been studied by first principles calculations[11, 12], and by a simplified effective Hubbard model [13–19] described by a hopping parameter  $t$  and a site-local repulsion  $U$ . Ref. 15 showed that the magnetism in graphene is robust to “shape disorder” of the nanostructure, while ref. 17 studied finite width graphene nanoribbons including the effects of doping. There are also studies of defect induced magnetism[20, 21] and of magnetism of other nanostructures[14, 22]. There are encouraging recent experimental signatures of magnetism[23–25], along with suggestions[26] that extraneous effects such as reconstruction would render the magnetism fragile.

The origin of magnetic moment in zigzag edge terminated honeycomb nanostructures has been attributed to the edge states[2, 27, 28] - localized electronic states which have most weight at the edges and die exponentially in the bulk.[29–31] These states are of topological origin[32] and have been experimentally observed using scanning tunneling microscopy.[33, 34] Magnetism at the edges is attributed to the Stoner mechanism(see, e.g., [35]) and is best discussed in terms of a Landau theory.[35] The ground state energy of the system is ex-

pressed as

$$E(\mathbf{M}) = a(U_c - U)|\mathbf{M}|^2 + b|\mathbf{M}|^4 + \dots \quad (1)$$

where  $\mathbf{M}$  is the magnetic order parameter,  $a, b > 0$  are positive constants that depend on the microscopics, and  $U_c$  is a critical value of the on-site repulsion. For  $U < U_c$ , the energy is minimum when  $\mathbf{M} = \mathbf{0}$ , i. e., system is non-magnetic. At  $U = U_c$ , there is a quantum phase transition to the magnetic state, and for  $U > U_c$  one finds  $|\mathbf{M}| \sim \sqrt{U - U_c}$ . Stoner theory[36], based on linear response formulation, provides an expression for  $U_c \sim \frac{1}{g(\varepsilon_F)}$ , where  $g(\varepsilon_F)$  is density of states of the bare system ( $U = 0$ ) at the zero temperature chemical potential  $\varepsilon_F$ . Thus for a zigzag edge terminated system,  $U_c$  would vanish, since the density of states  $g(\varepsilon_F)$  diverges owing to the non dispersive nature of the edge states. The Stoner-Landau theory would therefore suggest that a zigzag edge will have spontaneous magnetization  $\mathbf{M}$  for any  $U > 0$ , and furthermore that  $|\mathbf{M}| \sim \sqrt{U}$  for  $U \ll t$ .

It is known[37] that a zigzag edge terminated nanoribbon has a highly nonlinear response akin to that of sensory organs like eyes and ears. Their density response depends *logarithmically* on the magnitude of an edge potential applied at the zigzag edges. In this paper we show that such a Weber-Fechner response[38] of these nanoribbons plays a central role in determining their magnetism. Our work leads to a “magnetic phase diagram” of lightly doped nanoribbons, including analytical expressions for the width  $W$  and  $U$  dependence of the magnetization, excitation gap, and the critical doping required to engender magnetic transitions. We also corroborate these results with variational quantum Monte Carlo calculations and show that the magnetism is robust to fluctuations. To the best of our knowledge, this is the first report that

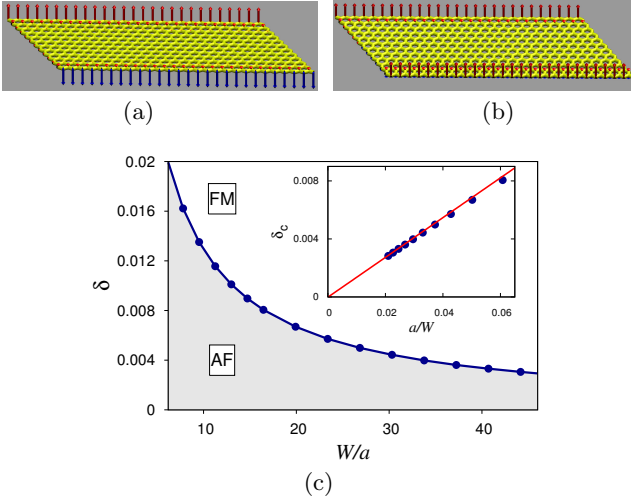


FIG. 1. (color online) Two possible magnetic states of zigzag-edged nanoribbon, (a) antiferromagnetic (AF) and (b) ferromagnetic (FM). (c) Magnetic phase diagram of zigzag nanoribbons for  $U = 1.5$  obtained from numerical mean field calculations. Inset: the critical doping required for AF to FM transition is inversely proportional to the ribbon width.

clearly points out that the usual Stoner-Landau theory is inadequate to understand magnetism of hexagonal lattice nanoribbons. This gains added significance in view of recent developments of cold atom optical lattices,[39] where honeycomb lattices have been realized and studied.[40]

The simplest Hamiltonian that describes the energetics of interacting electrons in the honeycomb lattice is the Hubbard model

$$H = -t \sum_{\langle ij \rangle, \sigma} c_{i\sigma}^\dagger c_{j\sigma} + U e_0 \sum_i n_{i\uparrow} n_{i\downarrow} - \mu \sum_i n_{i\sigma} \quad (2)$$

where  $c_{i\sigma}^\dagger$  is the operator that creates an electron of spin  $\sigma$  at site  $i$ ,  $n_{i\sigma} = c_{i\sigma}^\dagger c_{i\sigma}$  is the number operator,  $t$  is the nearest neighbour hopping amplitude,  $U e_0$  is the on-site Hubbard repulsion ( $e_0 = \frac{\sqrt{3}}{2}t$  is a characteristic energy scale,  $U$  is dimensionless), and  $\mu$  is the chemical potential. The underlying triangular Bravais lattice has a lattice parameter  $a$ , and the width of the the zigzag edge terminated nanoribbon is denoted by  $W$ .

Ground state of the zigzag edge terminated ribbon is obtained by a mean field analysis, where the four fermion interaction term is treated in the “magnetic channel” via the ansatz  $n_{i\uparrow} n_{i\downarrow} \rightarrow \frac{1}{2} N_i \sum_\sigma n_{i\sigma} + M_i S_i^z - (\frac{1}{4} N_i^2 - M_i^2)$ , where  $S_i^z = \frac{1}{2} (n_{i\uparrow} - n_{i\downarrow})$ ,  $N_i = \langle \sum_\sigma n_{i\sigma} \rangle$  is the mean occupancy, and  $M_i = \langle S_i^z \rangle$  is the local magnetization at site  $i$ . The quantities  $N_i$  and  $M_i$  are to be determined by enforcing the self consistency conditions of the mean field theory. Our detailed numerical calculation exploits translational symmetry along the nanoribbon (see Fig. 1(a)) where we have used up to 4000 equally spaced points to sample the 1D Brillouin zone. Fig. 1 shows the results for the values of physical parameters typical for

graphene. We find that there are two possible magnetic configurations where the moments along the two edges of nanoribbon are oppositely aligned (the anti-ferro (AF) configuration, see Fig. 1(a)) and aligned in the same direction (the ferro (FM) configuration, see Fig. 1(b)). For both these configurations, the moments are concentrated on the sites at the edge layers – this point will be important in the discussion below. At half-filling (one electron per site), the ground state has an AF structure consistent with earlier results[11]. With the doping of holes denoted by  $\delta$  ( $\delta$  is defined as the doping per edge atom of the ribbon), the ground state changes to the FM configuration at a critical doping[17]. This critical doping  $\delta_c$  required for the first order transition is dependent on the width of the ribbon and we find that  $\delta_c \sim \frac{a}{W}$  as shown in Fig. 1(c), the “magnetic phase diagram”. In the remainder of the paper, we develop an analytical theory of the physics behind this phase diagram.

The continuum field theory[41] that captures the physics of the Hamiltonian eqn. (2) has the action ( $\hbar = 1$ )

$$\mathcal{S}[\Psi] = \int d^{2+1}r \sum_\sigma \Psi_\sigma^*(r) (\mathbb{1} \partial_\tau + \mathcal{H}_K) \Psi_\sigma(r) + U e_0 a^2 \int d^{2+1}r \left[ \frac{1}{4} n(r)^2 - \{s^z(r)\}^2 \right] \quad (3)$$

where  $r = (\mathbf{r}, \tau)$ ,  $\mathbf{r} \equiv (x, y)$  is the position vector where  $x$ -coordinate is along the length of the ribbon and  $y$  along the width,  $\tau$  is the imaginary time that runs from 0 to  $\beta$  (inverse temperature),  $\Psi_\sigma^* = (\psi_{A+\sigma}^* \psi_{B+\sigma}^* \psi_{A-\sigma}^* \psi_{B-\sigma}^*)$  is the array of Grassmann fields with  $A/B$  and  $+/-$  being, respectively, sublattice and valley indices,  $n(r) = \sum_{a\nu\sigma} \psi_{a\nu\sigma}^*(r) \psi_{a\nu\sigma}(r)$  is the number density,  $s^z(r) = \frac{1}{2} \sum_{a\nu\sigma} \sigma \psi_{a\nu\sigma}^*(r) \psi_{a\nu\sigma}(r)$  is the spin density,  $\mathbb{1}$  is the  $4 \times 4$  identity matrix, and

$$\mathcal{H}_K = v_F \begin{pmatrix} \boldsymbol{\tau} \cdot \mathbf{P} & \mathbf{0} \\ \mathbf{0} & -\boldsymbol{\tau}^* \cdot \mathbf{P} \end{pmatrix} - \mu \mathbb{1} \quad (4)$$

with  $v_F = e_0 a$ , and  $\mathbf{P} = -i\nabla$ , the momentum operator,  $\boldsymbol{\tau} = \tau_x \mathbf{e}_x + \tau_y \mathbf{e}_y$  ( $\tau_{x,y}$  – Pauli matrices in the sublattice space,  $\mathbf{e}_{x,y}$  are spatial basis vectors). The action, written in a form that anticipates magnetism, can be studied by introducing a Hubbard-Stratanovich field  $m(r)$  to decouple the  $(s^z)^2$  term in eqn. (3), while the  $n^2$  term can be treated in a straightforward manner via a Hartree shift. The action becomes

$$\mathcal{S}[\Psi, m] = \int d^{2+1}r \sum_\sigma \Psi_\sigma^*(r) (\mathbb{1} \partial_\tau + \mathcal{H}_K) \Psi_\sigma(r) + \int d^{2+1}r \left[ m(r) s^z(r) + \text{g.c.} + \frac{1}{U e_0 a^2} |m(r)|^2 \right] \quad (5)$$

which upon integration of the fermion fields yields

$$\mathcal{S}[m] = \ln \prod_\sigma \det(-G_\sigma^{-1}[m]) + \frac{1}{U e_0 a^2} \int d^{2+1}r |m(r)|^2, \quad (6)$$

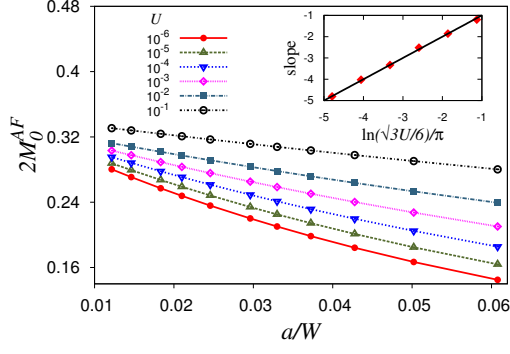


FIG. 2. (color online) (a) Width dependence of magnetic moment of the AF configuration for different values of  $U$  obtained from the full numerical solution compared with the analytical result eqn. (11). Inset: The logarithmic dependence of the slope of  $M_0^{AF}$  vs.  $a/W$  on  $U$  – points are obtained from the numerical simulations, solid line is from eqn. (11).

where the inverse Green's function is given by  $-G_\sigma^{-1}(r, r', m) = [\mathbb{1}\partial_\tau + \mathcal{H}_K + \frac{\sigma}{2}\{m(r) + m^*(r)\}\mathbb{1}]\delta(r - r')$ . The magnetic ground state of the system can be described by a saddle point of the action eqn. (6). The saddle point field  $m_s$  satisfies the condition

$$\frac{1}{Ue_0a^2}m_s(r) = \sum_\sigma \frac{\sigma}{2}G_\sigma(r, r; m_s). \quad (7)$$

We consider two different saddle point ansatzes for the undoped nanoribbons. For the AF configuration, we have

$$m_s^{AF}(y) = Ue_0a^2 \left[ \frac{M^{AF}}{a}\delta_D(y - W) - \frac{M^{AF}}{a}\delta_D(y) \right] \quad (8)$$

where  $M^{AF}$  is the moment associated with one edge, and FM configuration has

$$m_s^{FM}(y) = Ue_0a^2 \left[ \frac{M^{FM}}{a}\delta_D(y - W) + \frac{M^{FM}}{a}\delta_D(y) \right], \quad (9)$$

where  $M^{FM}$  is, again, the moment associated with one edge, and  $\delta_D$  is the Dirac delta function. Solution of  $M^{AF}$  and  $M^{FM}$  is aided by the observation that the right hand side of eqn. (7) is the magnetic moment density response of a nanoribbon with applied edge Zeeman fields. As shown in ref. [37], this response is highly non-linear akin to that of sensory organs. Thus, for the AF configuration, eqn. (7) reduces to

$$M^{AF} = \frac{1}{2} \left[ \frac{1}{3} + \frac{a}{\pi W} \ln \left( \sqrt{3} U M^{AF} \right) \right] \quad (10)$$

For the FM configuration,  $M^{FM}$  satisfies a similar equation sans the factor of  $\sqrt{3}$  in front of  $U$ . For wide ribbons

$W \gg a$ , we find

$$M_0^{AF} \approx \frac{1}{2} \left[ \frac{1}{3} + \frac{a}{\pi W} \ln \left( \frac{\sqrt{3}U}{6} \right) \right] \quad (11)$$

$$M_0^{FM} \approx \frac{1}{2} \left[ \frac{1}{3} + \frac{a}{\pi W} \ln \left( \frac{U}{6} \right) \right] \quad (12)$$

in undoped case (hence the subscript 0). We further find that the AF configuration has a one-particle excitation gap given by

$$\frac{\varepsilon_g}{e_0} \approx -\frac{2a}{W} \left( \frac{U}{6} \right) \ln \left( \frac{U}{6} \right) \quad (13)$$

Fig. 2 presents a comparison of the analytical results for the AF configuration with the full numerical calculations. We find excellent *quantitative* agreement of the calculated edge moment with the theory (eqn. (11)) over five decades of  $U$  (see inset[42] of Fig. 2). Similar quantitative agreement is found for the energy gap eqn. (13). We also find excellent quantitative agreement between our theory and the numerical calculations of the FM state.

Our theory predicts the AF configuration to be the ground state of the undoped ribbons for any width. This owes to the fact that the edge moment  $M_0^{AF}$  is larger than  $M_0^{FM}$ ,

$$\Delta M_0 = M_0^{AF} - M_0^{FM} = \frac{\ln \sqrt{3}}{2\pi} \frac{a}{W} \quad (14)$$

which, remarkably, is independent of  $U$ . The difference in the ground state energies ( $E_0^{AF} - E_0^{FM}$ ) per unit repeat distance along the length of the ribbon is estimated as  $\frac{\Delta E_0}{e_0} \approx -U \left[ \frac{\ln \sqrt{3}}{3} \frac{a}{\pi W} + \left( \frac{(\ln \sqrt{3})^2}{2} + \frac{(6-\pi) \ln \sqrt{3}}{6} \ln \left( \frac{U}{6} \right) \right) \left( \frac{a}{\pi W} \right)^2 \right]$ , where the leading term in  $a/W$  arises from the correlation energy (proportional to  $M^2$ ), and the second term  $\sim (a/W)^2$  also contains the kinetic energy of the electrons in the effective bands. The ground state of the undoped system is always the AF configuration the physics of which traces back to the sensory organ like response of zigzag-edge terminated ribbons.

Upon doping the system with holes ( $\delta > 0$ ) or electrons ( $\delta < 0$ ), the edge magnetization changes. For the AF configuration, we find

$$M^{AF}(\delta) = M_0^{AF} - \frac{|\delta|}{2} \quad (15)$$

while, interestingly, for the FM configuration

$$M^{FM}(\delta) \approx M_0^{FM} - s(U) \frac{W}{a} \delta^2 \quad (16)$$

where  $s(U) \approx \frac{\pi}{4} \left( 1 + \frac{2}{\ln(U/6)} \right)$ . This leads to an energy difference between the two states

$$\Delta E(\delta) = -\frac{2Ue_0}{3} \left( \Delta M_0 - \frac{|\delta|}{2} + s(U) \frac{W}{a} \delta^2 \right) \quad (17)$$

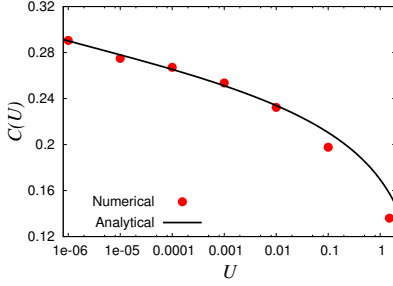


FIG. 3. (color online) Dependence of  $C(U)$  on  $U$ . Critical doping  $\delta_c$  for transition from AF to FM state is given by  $\delta_c = C(U) \frac{a}{W}$  (see eqn. (18)).

to order  $a/W$ . We see that a first order transition from the AF to the FM configuration occurs at a critical doping

$$\delta_c = C(U) \frac{a}{W}, \quad C(U) = \frac{1 - \sqrt{1 - \ln 3 \left(1 + \frac{2}{\ln(U/6)}\right)}}{\pi \left(1 + \frac{2}{\ln(U/6)}\right)} \quad (18)$$

Fig. 3 shows a comparison of this analytical result eqn. (18) with the numerical values of  $C(U)$ , and again, excellent quantitative agreement is found over many decades of  $U$ . For larger values of  $U$  (such as that found in graphene), we find quantitative agreement up to about 10%. This owes to the fact that larger values of  $U$  results in a small contribution from the bulk states, which is not captured in our edge mode based analytical theory. To the best of our knowledge, this is the first analytical and quantitative theory of the magnetism in zigzag-edged ribbons. An important point brought about by the theory is that interpreting the magnetism in these systems via a Stoner-Landau theory of the form eqn. (1) may be too simplistic. Indeed, the energy functional has a non-analytic structure  $E(M) = AM^2 + BM \ln DM$  ( $A, B, D$  constants), that has roots in the sensory organ like Weber-Fechner response of zigzag-edge ribbons.

It is important to ensure that quantum fluctuations does not change the qualitative physics uncovered by the analytical theory. To this end, we performed variational Monte Carlo calculations of the ground state. Our trial wave function  $|\Psi\rangle = g^D |FS, M\rangle$ , where  $D$  is the double occupancy operator,  $g$  is a the Gutzwiller factor that penalises double occupancy,  $|FS, M\rangle$  is the filled Fermi sea state constructed by imposing an edge magnetization  $M$  on the edge layers. For the AF configuration  $M$  has opposite site on the two edges while for the FM configuration  $M$  is equal on both edges. The optimal values of  $g$  and  $M$  are obtained so as to minimize the ground state energy. We have studied ribbons with  $W \approx 6a$  with  $U = 1.5$ . We find that the ground state at zero doping is the AF configuration, with an edge moment 0.20 which is expectedly smaller than the mean field value 0.27 owing to quantum fluctuations. Furthermore, the ground state changes to FM configuration at a critical doping  $\delta$  of

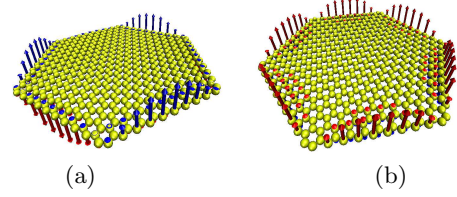


FIG. 4. (color online) (a) Mean-field AF configuration in a zigzag edge terminated hexagonal nanodot ( $U = 1.5$ ) (b) FM configuration obtained upon doping ( $\delta = 0.1$ ).

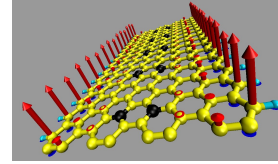


FIG. 5. (color online) FM structure of the boron substituted zigzag edge terminated graphene nanoribbon obtained from first principles calculations. Dark atoms are borons and light ones are carbon. Hydrogen passivation of the edge atoms is also shown.

0.025. Both the AF and FM edge moments are stable, in that they remain unchanged upon increasing the length of the ribbon (for a given width  $W$ ), proving that the magnetism is robust. While these calculations are prohibitively expensive for the determination the full phase diagram, these results provide evidence for the correctness of our analytical theory.

We have further investigated other zig-zag edge terminated nanostructures. For a undoped hexagonal nanodot, we find that the magnetic configuration has an AF structure[14] as shown in Fig. 4(a), which upon doping, changes to a FM type (see Fig. 4(b)). Doping in practical applications can be achieved by gating. We have also explored possible chemical modification of graphene nanoribbons to produce an “internal doping” to engender the magnetic transition. Fig. 5 shows a FM structure of a zigzag edge terminated nanoribbon[43] with boron atoms substituted[44] in place of carbons, while the undoped nanoribbon has a AF configuration within the same calculation. As is evident, the results of this paper suggest many interesting possibilities of using zigzag edge terminated graphene nanostructures in applications.

AM thanks CPDF, IISc for support. VBS is grateful to DST for Ramanujan and MONAMI grants, and DAE-SRC for generous support. The authors thank Umesh Waghmare for help with the first principles calculations, R. Shankar and Jayantha Vyasanakere for discussions.

\* bsomnath@mrc.iisc.ernet.in

† amedhi@physics.iisc.ernet.in

<sup>†</sup> shenoy@physics.iisc.ernet.in

- [1] R. M. Westervelt, *Science* **320**, 324 (2008).
- [2] A. H. C. Neto, F. Guinea, N. M. R. Peres, K. S. Novoselov, and A. K. Geim, *Rev. Mod. Phys.* **81**, 109 (2009).
- [3] S. K. Pati, T. Enoki, and C. N. R. Rao, eds., *Graphene and its fascinating attributes* (World Scientific, 2011).
- [4] J. Bunch, Y. Yaish, M. Brink, K. Bolotin, and P. McEuen, *Nano Lett.* **5**, 287 (2005).
- [5] F. Miao, S. Wijeratne, Y. Zhang, U. C. Coskun, W. Bao, and C. N. Lau, *Science* **317**, 1530 (2007).
- [6] L. A. Ponomarenko, F. Schedin, M. I. Katsnelson, R. Yang, E. W. Hill, K. S. Novoselov, and A. K. Geim, *Science* **320**, 356 (2008).
- [7] J. Wurm, M. Wimmer, I. Adagideli, K. Richter, and H. U. Baranger, *New Journal of Physics* **11**, 095022 (2009).
- [8] V. N. Kotov, B. Uchoa, V. M. Pereira, F. Guinea, and A. H. Castro Neto, *ArXiv e-prints* (2010), arXiv:1012.3484 [cond-mat.str-el].
- [9] Z. Y. Meng, T. C. Lang, S. Wessel, F. F. Assaad, and A. Muramatsu, *Nature* **464**, 847 (2010).
- [10] S. Pathak, V. B. Shenoy, and G. Baskaran, *Phys. Rev. B* **81**, 085431 (2010).
- [11] Y. W. Son, M. L. Cohen, and S. G. Louie, *Phys. Rev. Lett.* **97**, 216803 (2006).
- [12] Y. W. Son, M. L. Cohen, and S. G. Louie, *Nature (London)* **444**, 347 (2006).
- [13] N. M. R. Peres, M. A. N. Araújo, and D. Bozi, *Phys. Rev. B* **70**, 195122 (2004).
- [14] J. Fernandez-Rossier and J. J. Palacios, *Phys. Rev. Lett.* **99**, 177204 (2007).
- [15] S. Bhowmick and V. B. Shenoy, *The Journal of Chemical Physics* **128**, 244717 (2008).
- [16] O. V. Yazyev, *Phys. Rev. Lett.* **101**, 037203 (2008).
- [17] J. Jung and A. H. MacDonald, *Phys. Rev. B* **79**, 235433 (2009).
- [18] T. Ma, F. Hu, Z. Huang, and H.-Q. Lin, *Applied Physics Letters* **97**, 112504 (2010).
- [19] O. V. Yazyev, *Reports on Progress in Physics* **73**, 056501 (2010).
- [20] Y. Zhang, S. Talapatra, S. Kar, R. Vajtai, S. K. Nayak, and P. M. Ajayan, *Phys. Rev. Lett.* **99**, 107201 (2007).
- [21] O. V. Yazyev and L. Helm, *Phys. Rev. B* **75**, 125408 (2007).
- [22] M. Ezawa, *Phys. Rev. B* **76**, 245415 (2007).
- [23] H. S. S. Ramakrishna Matte, K. S. Subrahmanyam, and C. N. R. Rao, *ArXiv e-prints* (2009), arXiv:0904.2739 [physics.chem-ph].
- [24] C. N. R. Rao, H. S. S. R. Matte, K. S. Subrahmanyam, and U. Maitra, *Chem. Sci.* **3**, 45 (2012).
- [25] V. L. J. Joly, M. Kiguchi, S.-J. Hao, K. Takai, T. Enoki, R. Sumii, K. Amemiya, H. Muramatsu, T. Hayashi, Y. A. Kim, M. Endo, J. Campos-Delgado, F. López-Urías, A. Botello-Méndez, H. Terrones, M. Terrones, and M. S. Dresselhaus, *Phys. Rev. B* **81**, 245428 (2010).
- [26] J. Kunstmann, C. Özdoğan, A. Quandt, and H. Fehske, *Phys. Rev. B* **83**, 045414 (2011).
- [27] K. Nakada, M. Fujita, G. Dresselhaus, and M. S. Dresselhaus, *Phys. Rev. B* **54**, 17954 (1996).
- [28] K. Wakabayashi, M. Fujita, H. Ajiki, and M. Sigrist, *Phys. Rev. B* **59**, 8271 (1999).
- [29] L. Brey and H. A. Fertig, *Phys. Rev. B* **73**, 195408 (2006).
- [30] L. Brey and H. A. Fertig, *Phys. Rev. B* **73**, 235411 (2006).
- [31] M. Zarea and N. Sandler, *Phys. Rev. B* **79**, 165442 (2009).
- [32] S. Ryu and Y. Hatsugai, *Phys. Rev. Lett.* **89**, 077002 (2002).
- [33] Y. Kobayashi, K. Fukui, T. Enoki, K. Kusakabe, and Y. Kaburagi, *Phys. Rev. B* **71**, 193406 (2005).
- [34] Y. Niimi, T. Matsui, H. Kambara, K. Tagami, M. Tsukada, and H. Fukuyama, *Phys. Rev. B* **73**, 085421 (2006).
- [35] A. Altland and B. Simons, *Condensed Matter Field Theory* (Cambridge University Press, 2006).
- [36] K. Yosida, *Theory of Magnetism* (Springer-Verlag, 1996).
- [37] S. Bhowmick and V. B. Shenoy, *Phys. Rev. B* **82**, 155448 (2010).
- [38] See [http://en.wikipedia.org/wiki/Weber-Fechner\\_law](http://en.wikipedia.org/wiki/Weber-Fechner_law).
- [39] I. Bloch, J. Dalibard, and S. Nascimbene, *Nat. Phys.* **8**, 267 (2012).
- [40] L. Tarruell, D. Greif, T. Uehlinger, G. Jotzu, and T. Esslinger, *Nature* **483**, 302 (2012).
- [41] I. F. Herbut, *Phys. Rev. Lett.* **97**, 146401 (2006).
- [42] The slope in the inset of Fig. 2 is the coefficient of the linear term obtained by fitting a polynomial  $M(a/W) = c_0 + c_1(a/W) + c_2(a/W)^2$ .
- [43] These calculations were done using Quantum Espresso code,[45] using plane-wave basis set and ultrasoft pseudo-potential. The energy cutoff for the plane-wave basis for wavefunctions is set to be 40 Ry. Electron exchange-correlation is treated with a local density approximation(LDA, Perdew-Zunger functional). Nanoribbons are simulated using a supercell geometry, with a vacuum layer of 15Å between any two periodic images of the ribbon. A k-point grid of 24x1x1 k points (periodic direction of the ribbon along x-axis) is used for sampling Brillouin zone integrations for this geometry.
- [44] L. S. Panchakarla, K. S. Subrahmanyam, S. K. Saha, A. Govindaraj, H. R. Krishnamurthy, U. V. Waghmare, and C. N. R. Rao, *Advanced Materials* **21**, 4726 (2009).
- [45] P. Giannozzi, S. Baroni, N. Bonini, M. Calandra, R. Car, C. Cavazzoni, D. Ceresoli, G. L. Chiarotti, M. Cococcioni, I. Dabo, A. Dal Corso, S. de Gironcoli, S. Fabris, G. Fratesi, R. Gebauer, U. Gerstmann, C. Gougoussis, A. Kokalj, M. Lazzeri, L. Martin-Samos, N. Marzari, F. Mauri, R. Mazzarello, S. Paolini, A. Pasquarello, L. Paulatto, C. Sbraccia, S. Scandolo, G. Sclauzero, A. P. Seitsonen, A. Smogunov, P. Umari, and R. M. Wentzcovitch, *Journal of Physics: Condensed Matter* **21**, 395502 (19pp) (2009).